Anal. Chem. **2004,** *76,* 6651−6658

Depth Profiling of Langmuir−Blodgett Films with a Buckminsterfullerene Probe

Audra G. Sostarecz,† Carolyn M. McQuaw,† Andreas Wucher,‡ and Nicholas Winograd*,†

Department of Chemistry, The Pennsylvania State University, 104 Chemistry Building, University Park, Pennsylvania 16802, and Department of Physics, University of Duisburg-Essen, 45117 Essen, Germany

Bombardment with C_{60}^+ primary ions of monolayer and multilayer barium arachidate Langmuir−Blodgett (LB) films is investigated. The behavior of cluster versus atomic (Ga^+) bombardment is monitored by the barium-cationized arachidate ion (mass-to-charge ratio (*m/z*) 449) and a characteristic fragment ion (*m/z* 209) using 1-, 7-, and 15-layer model systems. The removal rate of material from the films is shown to be on the order of several hundred molecules per C_{60} impact, a value 100-fold larger than Ga^+ impact. The enhancement in secondary ion yield is also shown to be larger for the 15-layer film (400×) than for the monolayer film (100×). Moreover, most of the increase in yield is shown to be associated with ejection of sputtered species rather than an increase in ionization probability. High yields associated with cluster bombardment are also shown to be amenable to depth profiling experiments in which the two ions can be monitored as the film is being removed. In this modality, chemical damage associated with bombardment is removed before it can accumulate on the surface. Due to the similarity of fatty acid LB films to cellular membranes, these results suggest that C_{60}^+ primary ion beams may improve the prospects for TOF-SIMS studies of biological systems.

Cluster ion beams are becoming popular as primary ion sources for the study of complex organic thin films by secondary ion mass spectrometry (SIMS). These sources are reviving interest in SIMS, since they largely overcome previous difficulties associated with low secondary ion intensity and accumulated beam-induced damage characteristic of corresponding atomic projectiles. These cluster sources include species consisting of $SF_6^{0,-}$,[1] Au_n^+,[2−6] metal oxides,[7] SF_5^+,[8−13] small carbon clusters,[13,14] and C_{60}^+.[15−24] In virtually every circumstance, the yield of organic molecular ions is significantly enhanced. Moreover, in selected cases, the cluster projectile removes material with a lower damage cross section, yielding higher detection efficiencies.[17] Perhaps most importantly, for materials exhibiting very high sputter rates, the accumulated damage appears to be removed as fast as it is created, thus opening the possibility of molecule-specific depth profiling. This modality has now been demonstrated using SF_5^+ to bombard amino acid[10] and polymer thin film[10−12] substrates.

Recently, a robust buckminsterfullerene (C_{60}^+) ion beam system has been reported for time-of-flight (TOF) SIMS experiments.[16,17] This projectile appears to provide the best mass spectral performance of any SIMS source yet examined, with applications to protein assay and sequencing as well as bioimaging[18,19] and molecular depth profiling already reported.[20−22] This cluster source is effective, since at 20 keV impact energy, each carbon atom has only 333 eV of kinetic energy. The simultaneous interaction of 60 of these carbon atoms with the target allows very efficient energy transfer into the molecular desorption channel. It has been reported, for example, that several thousand water molecules are removed from an ice film for each C_{60}^+ impact.[24]

* To whom correspondence should be addressed. Telephone: (814) 863-0001. Fax: (814) 863-0618. E-mail: nxw@psu.edu.

† The Pennsylvania State University.

‡ University of Duisburg-Essen.

(1) Appelhans, A. D.; Delmore, J. E. *Anal. Chem.* **1989**, *61*, 1087−1093.
(2) Benguerba, M.; Brunelle, A.; Della-Negra, S.; Depauw, J.; Joret, H.; Le Beyec, Y.; Blain, M. G.; Schweikert, E. A.; Ben Assayag, G.; Sudraud, P. *Nucl. Instrum. Methods Phys. Res., Sect. B* **1991**, *62*, 8−22.
(3) Davies, N.; Weibel, D. E.; Blenkinsopp, P.; Lockyer, N.; Hill, R.; Vickerman, J. C. *Appl. Surf. Sci.* **2003**, *203−204*, 223−227.
(4) Boussofiane-Baudin, K.; Bolbach, G.; Brunelle, A.; Della-Negra, S.; Håkansson, P.; Le Beyec, Y. *Nucl. Instrum. Methods Phys. Res., Sect. B* **1994**, *88*, 160−163.
(5) Walker, A. V.; Winograd, N. *Appl. Surf. Sci.* **2003**, *203−204*, 198−200.
(6) Touboul, D.; Halgand, F.; Brunelle, A.; Kersting, R.; Tallarek, E.; Hagenhoff, B.; Laprévote, O. *Anal. Chem.* **2004**, *76*, 1550−1559.
(7) Harris, R. D.; Van Stipdonk, M. J.; Schweikert, E. A. *Int. J. Mass Spectrom. Ion Processes* **1998**, *174*, 167−177.
(8) Kötter, F.; Benninghoven, A. *Appl. Surf. Sci.* **1998**, *133*, 47−57.
(9) Stapel, D.; Brox, O.; Benninghoven, A. *Appl. Surf. Sci.* **1999**, *140*, 156−167.
(10) Gillen, G.; Roberson, S. *Rapid Commun. Mass Spectrom.* **1998**, *12*, 1303−1312.
(11) Fuoco, E. R.; Gillen, G.; Wijesundara, M. B. J.; Wallace, W. E.; Hanley, L. *J. Phys. Chem. B* **2001**, *105*, 3950−3956.
(12) Wagner, M. S. *Anal. Chem.* **2004**, *76*, 1264−1272.
(13) Gillen, G.; Fahey, A. *Appl. Surf. Sci.* **2003**, *203−204*, 209−213.
(14) Gillen, G.; King, L.; Freibaum, B.; Lareau, R.; Bennett, J.; Chmara, F. *J. Vac. Sci. Technol., A* **2001**, *19*, 568−575.
(15) Van Stipdonk, M. J.; Harris, R. D.; Schweikert, E. A. *Rapid Commun. Mass Spectrom.* **1996**, *10*, 1987−1991.
(16) Wong, S. C. C.; Hill, R.; Blenkinsopp, P.; Lockyer, N. P.; Weibel, D. E.; Vickerman, J. C. *Appl. Surf. Sci.* **2003**, *203−204*, 219−222.
(17) Weibel, D.; Wong, S.; Lockyer, N.; Blenkinsopp, P.; Hill, R.; Vickerman, J. C. *Anal. Chem.* **2003**, *75*, 1754−1764.
(18) Xu, J.; Ostrowski, S.; Ewing, A. G.; Winograd, N. *Appl. Surf. Sci.* **2004**, *231−232*, 159−163.
(19) Xu, J.; Szakal, C. W.; Martin, S. E.; Peterson, B. R.; Wucher, A.; Winograd, N. *J. Am. Chem. Soc.* **2004**, *126*, 3902−3909.
(20) Szakal, C.; Sun, S.; Wucher, A.; Winograd, N. *Appl. Surf. Sci.* **2004**, *231−232*, 183−185.
(21) Wucher, A.; Sun, S.; Szakal, C.; Winograd, N. *Appl. Surf. Sci.* **2004**, *231−232*, 68−71.
(22) Sostarecz, A. G.; Sun, S.; Szakal, C.; Wucher, A.; Winograd, N. *Appl. Surf. Sci.* **2004**, *231−232*, 179−182.
(23) Sun, S.; Szakal, C.; Smiley, E. J.; Postawa, Z.; Wucher, A.; Garrision, B. J.; Winograd, N. *Appl. Surf. Sci.* **2004**, *231−232*, 64−67.
(24) Wucher, A.; Sun, S.; Szakal, C.; Winograd, N. *Anal. Chem.*, in press.

10.1021/ac0492665 CCC: $27.50
Published on Web 10/09/2004

Here, we examine the response of monolayer and multilayer Langmuir−Blodgett (LB) films of barium arachidate to C_{60}^+ bombardment. LB fatty acid salt films provide a highly ordered, stable, and reproducible surface for measurement.[25,26] LB fatty acid and fatty acid salt films have been extensively employed in SIMS studies.[9,22,27−35] Some of these studies involve investigating ion beam dosage effects by monitoring the organic molecular ion.[9,28,29] Other studies have investigated the chemical effects of sputter-depth profiling with alternating metal multilayered fatty acid salt LB films. The atomic secondary metal ions that form the fatty acid salts were monitored in these studies, rather than the organic molecular secondary ions that could provide more specific chemical information.[30]

Our results show that the secondary ion yield of the molecular ion and a characteristic ion of monolayer and 7- and 15-layer films is enhanced 2 orders of magnitude when compared to Ga^+ bombardment of comparable impact energy. As expected, the removal rate of molecules from a 7-layer LB film is also enhanced by ~2 orders of magnitude in comparison to atomic bombardment. From the known thickness of the film and the known dose required to remove it from the silicon substrate, we show that the observed secondary ion yield enhancement arises primarily from an increased sputter yield rather than from any enhancement associated with the ionization probability of the secondary ions. Finally, we show that for the 7- and 15-layer LB films, the barium-cationized arachidate ion at a mass-to-charge ratio (m/z) of 449 and a prominent fragment ion at m/z 209 can be directly monitored during a depth profiling experiment. Although some chemical damage is observed for the m/z 449 component, results on both the 7- and 15-layer films suggest that we are approaching the experimental conditions that give rise to a zero damage regime, even for these rather long chain hydrocarbon species. The profiles are discussed in terms of understanding the behavior of cluster ion bombardment of thin film structures. These results have implications for the utilization of a C_{60}^+ primary ion source for the depth profiling of cells because the molecules in LB fatty acid films have a structure, orientation, and molecular area similar to those found in biological membranes.

EXPERIMENTAL SECTION

Materials. Arachidic acid, barium chloride (99.999%), potassium hydrogen carbonate (99.7%), and copper (II) chloride (99.999%) were purchased from Sigma-Aldrich (Allentown, PA) and used without further purification. Hexane and 2-propanol were also used without further purification for solvation of the arachidic acid. The water used in preparation of all LB films was purified from a Millipore Milli-Q System (Burlington, MA) and had a resistivity of 18.2 MΩ-cm with an organic content of 4 ppb.

Substrate and LB Film Preparation. Single crystal (100) silicon substrates were cut from 3-in. wafers. All Si substrates were cleaned by piranha etch (3:1 H_2SO_4/H_2O_2) and rinsed with high-purity water in order to ensure a hydrophilic surface (SiO_2/Si). (*Extreme caution must be exercised when using piranha etch. An explosion-proof hood should be used.*) Monolayer and multilayer LB films of barium arachidate were made using a μTrough S LB (Kibron; Helsinki, Finland). Arachidic acid (1 mg/mL) in 3:2 hexane/2-propanol was added dropwise to the subphase. The subphase consisted of aqueous 10^{-4} M $BaCl_2$ and 10^{-4} M $KHCO_3$ for formation of the fatty acid salt and film stability[36] and 10^{-7} M $CuCl_2$ to aid in the deposition of a large number of layers.[25] The monolayer was allowed to equilibrate for ~10 min before compression began. Isotherms were achieved by surface pressure measurements using a Wilhelmy wire interfaced to a personal computer. Trough barriers were computer-controlled to allow for uniform compression of the fatty acid monolayer as well as to maintain constant feedback when depositing layers. Isotherms were taken at room temperature at a rate of 7 Å^2/molecule/min, and films were deposited at a constant pressure of 33 mN/m at a rate of 10 mm/min. An odd number of layers of barium arachidate were deposited onto SiO_2/Si substrates by vertical deposition. Approximately 10 min was allotted between successive depositions for complete drying of the substrate. Monolayer films of arachidic acid were made in the same manner as the fatty acid salt films in the absence of additional salts or buffers in the water subphase. A single wavelength (632.8 nm, 1-mm spot size, 70° incidence angle) Stokes ellipsometer LSE (Gaertner Scientific Corporation; Skokie, IL) was used to ensure deposition of layers and to measure the sample thickness. At least three spots were measured for reproducibility. The thickness of one layer was determined to be ~27 Å. This thickness along with the area/molecule of the film applied (20 Å^2/molecule) was used to calculate a density of 1.85 × 10^{21} molecules/cm^3. The mass density is comparable to that which is obtained for arachidic acid using the atom-fragment density estimation method[37,38] (1.92 × 10^{21} molecules/cm^3).

Instrumentation. LB films were analyzed with a TOF-SIMS instrument[39] equipped with both a 15-keV Ga^+ liquid metal ion source and a 20-keV C_{60}^+ effusive ion source[17] (both sources from Ionoptika; Southampton, U.K.). For each sample, experiments were performed at room temperature in delayed extraction mode

(25) Blodgett, K. B. *J. Phys. Chem.* **1937**, *41*, 975−984.
(26) Blodgett, K. B.; Langmuir, I. *Phys. Rev.* **1937**, *51*, 964−982.
(27) Bolbach, G.; Plissonnier, M.; Galéra, R.; Blais, J. C., Dufour, G.; Roulet, H. *Thin Solid Films* **1992**, *210/211*, 524−526.
(28) Wandass, J. H.; Schmitt, R. L.; Gardella, J. A., Jr. *Appl. Surf. Sci.* **1989**, *40*, 85−96.
(29) Cornelio-Clark, P. A.; Gardella, J. A., Jr. *Langmuir* **1991**, *7*, 2279−2286.
(30) Wittmaack, K.; Laxhuber, L.; Möhwald, H. *Nuc. Instrum. Methods Phys. Res., Sect. B* **1987**, *18*, 639−643.
(31) Laxhuber, L.; Möhwald, H.; Hashmi, M. *Int. J. Mass Spectrom. Ion Phys.* **1983**, *51*, 93−110.
(32) Hoshi, T.; Yamada, S.; Yoshida, S.; Watanabe, T.; Kudo, M. In *Secondary Ion Mass Spectrometry SIMS X*; Benninghoven, A., Hagenhoff, B., Werner, H. W., Eds.; John Wiley & Sons: New York, 1997; pp 255−258.
(33) Hoshi, T.; Yoshida, S.; Watanabe, T.; Ichinohe, Y.; Kudo, M. *Appl. Surf. Sci.* **1999**, *142*, 614−618.
(34) Bolbach, G.; Beavis, R.; Della-Negra, S.; Deprun, C.; Ens, W.; Le Beyec, Y.; Main, D. E.; Schueler, B.; Standing, K. G. *Nuc. Instrum. Methods Phys. Res., Sect. B* **1988**, *30*, 74−82.
(35) Li, J.-X.; Johnson, R. W., Jr.; Gardella, J. A., Jr. Secondary Ion Mass Spectrometry As Applied to Thin Organic and Polymeric Films. In *Characterization of Organic Thin Films*; Ulman, A., Fitzpatrick, L. E., Eds.; Butterworth-Heinemann: Boston, 1995; pp 193−212.
(36) Girard, K. P.; Quinn, J. A.; Vanderlick, T. K. *Thin Solid Films* **2000**, *371*, 242−248.
(37) Nelken, L. H. Densities of Vapors, Liquids and Solids. In *Handbook of Chemical Property Estimation Methods Environmental Behavior of Organic Compounds*; Lyman, W. J., Reehl, W. F., Rosenblatt, D. H., Eds.; McGraw-Hill: New York, 1982; Chapter 19.
(38) Immirzi, A.; Perini, B. *Acta Crystallogr.* **1977**, *33*, 216−218.
(39) Braun, R. M.; Blenkinsopp, P.; Mullock, S. J.; Corlett, C.; Willey, K. F.; Vickerman, J. C.; Winograd, N. *Rapid Commun. Mass Spectrom.* **1998**, *12*, 1246−1252.

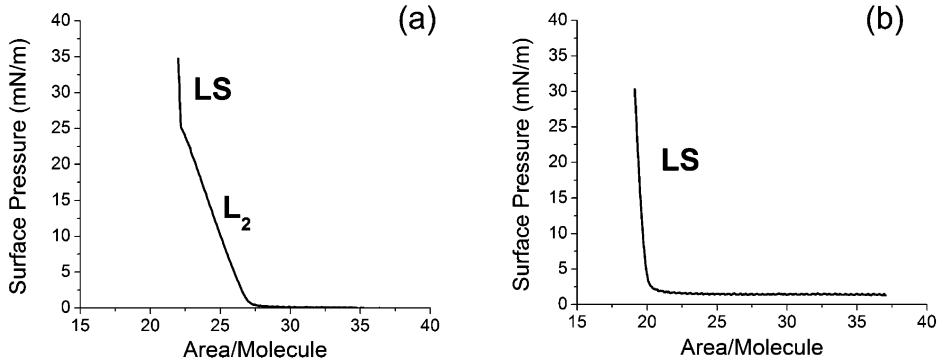

Figure 1. Surface pressure/area isotherms of (a) arachidic acid on a pure water subphase and (b) arachidic acid on a subphase consisting of 10^{-4} M $BaCl_2$, 10^{-4} M $KHCO_3$, and 10^{-7} M $CuCl_2$. Both isotherms were obtained at room temperature.

with a delay time of 100 ns between the primary ion pulse (duration 50 ns) and the secondary ion extraction pulse unless otherwise mentioned. Charge compensation was found to be unnecessary for positive SIMS mode.

For depth profiling, both beams (C_{60}^+ and Ga^+) were operated in DC mode to sputter-erode the surface at an area of $(500\ \mu m)^2$ and $(540\ \mu m)^2$, respectively. The C_{60}^+ erosion interval time was 5.8 s, which corresponds to a primary ion fluence of $\sim 8 \times 10^{12}$ cm^{-2}. The Ga^+ erosion interval times were 5.8, 50, and 100 s, resulting in primary ion fluences of $\sim 1.6 \times 10^{13}$ cm^{-2}, $\sim 1.4 \times 10^{14}$ cm^{-2}, and $\sim 2.8 \times 10^{14}$ cm^{-2}, respectively. Between erosion cycles, TOF spectra were taken with both C_{60}^+ and Ga^+ projectiles at low ion fluences of 10^{10} cm^{-2} at an area of $(300\ \mu m)^2$ for C_{60}^+ and $(250\ \mu m)^2$ for Ga^+ unless otherwise noted. In the determination of the C_{60}^+ ion fluence, a beam size of $\sim 100\ \mu m$ was accounted for. TOF mass spectra were acquired with an original time resolution of 1 ns with a flight time of 88.9 μs for the molecule-specific peak at a mass-to-charge ratio (m/z) of 449 and a typical peak width of ~40 ns. For better visibility of weak molecular features, all displayed spectra are binned to 20-ns time bins after acquisition. In all of the depth profile plots, the signal in counts/nC was determined by integrating the respective TOF peak and normalizing the integral to the total primary ion charge applied to acquire the spectrum.

RESULTS AND DISCUSSION

LB Film Surface Pressure/Area Isotherms. Stable multilayer LB films of long-chain fatty acids can be made with the addition of a salt to the subphase.[25,26] In this experiment, arachidic acid and a subphase consisting of $BaCl_2$ were used to produce barium arachidate, a salt of arachidic acid. Monolayer and multilayer (7 and 15 layers) films of barium arachidate were applied to a SiO_2/Si surface, with each molecule occupying an area of ~20 Å^2, corresponding to $\sim 5 \times 10^{14}$ molecules/cm^2. Representative surface pressure/area isotherms of arachidic acid on a pure water subphase and on a salt subphase are shown in Figure 1a and b, respectively. The absence of the L_2/LS phase transition in Figure 1b is an indication of conversion to the fatty acid salt.[40]

Mass Spectra. Positive TOF-SIMS analysis with a Ga^+ primary ion beam of a monolayer film of arachidic acid ($CH_3(CH_2)_{18}COOH$) deposited onto a hydrophilic silicon surface results in two

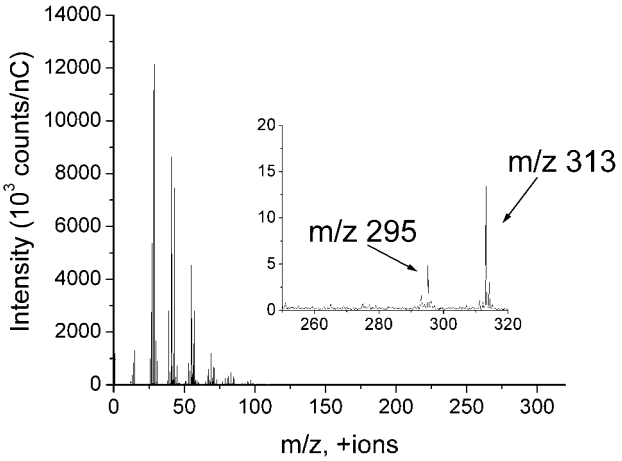

Figure 2. Ga^+-induced mass spectrum of a monolayer film of arachidic acid ($CH_3(CH_2)_{18}COOH$) depicting characteristic ions at m/z 295 $(M + H - 18)^+$ and m/z 313 $(M + H)^+$. The ion fluence is 10^{11} cm^{-2}, and the primary ion pulse has a duration of 17 ns. Spectrum was acquired without delayed extraction.

characteristic peaks at m/z 313 $(M + H)^+$ and m/z 295 $(M + H - 18)^+$ (Figure 2). A representative C_{60}^+-induced positive ion mass spectrum of a 15-layer film of barium arachidate is shown in Figure 3. Each barium arachidate LB film investigated in this study by C_{60}^+ bombardment produced the representative peaks depicted in Figure 3, regardless of the thickness of the film. Peaks specific to the fatty acid salt are found for the barium-cationized arachidate ion at m/z 449 for $CH_3(CH_2)_{18}COOBa^+$ and for a characteristic fragment, $CH_2CHCOOBa^+$, of this ion at m/z 209. The barium content of these peaks is identified from their representative Ba isotope pattern (Figure 3a). The occurrence of these ions is understandable, since there is a 1:2 binding stoichiometry for the metal cation with the fatty acid monolayer.[26] There is also a characteristic fragment peak at m/z 196 for CH_2COOBa^+; however, this peak is isobaric with the silicon cluster Si_7^+. A C_{60}^+ positive ion mass spectrum of the bare silicon surface after prolonged sputtering (Figure 4) demonstrates the appearance of many silicon cluster ions.

In the low-mass region, barium specific peaks are observed at m/z 138 for Ba^+, m/z 139 for $(Ba + H)^+$, and m/z 155 for $(BaOH)^+$ (Figure 3b). Clusters consisting of barium, oxygen, and/or carbon are also shown and identified as the following: m/z 163 $(BaC_2H)^+$, m/z 187 $(BaO_3H)^+$, m/z 211 $(BaO_3C_2H)^+$ (labeled with asterisks in Figure 3a), m/z 292 $(Ba_2O)^+$, m/z 309 $(Ba_2O_2H)^+$, and m/z 317 $(Ba_2OC_2H)^+$ (Figure 3c). All of these clusters have

(40) Kurnaz, M. L.; Schwartz, D. K. *J. Phys. Chem.* **1996**, *100*, 11113−11119.

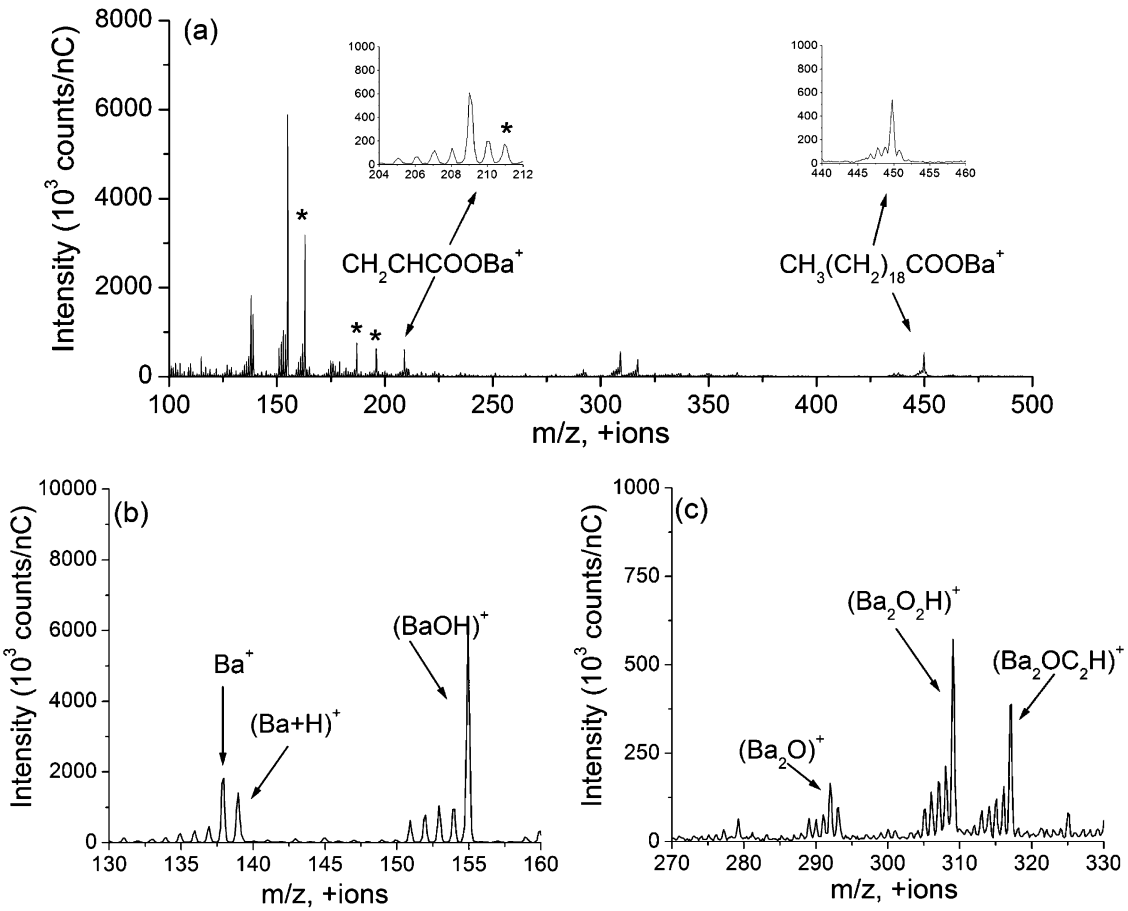

Figure 3. C_{60}^+-induced mass spectrum of a 15-layer LB film of barium arachidate: (a) the characteristic ions of the barium arachidate film at *m*/*z* 209 and 449 with their isotope patterns, as well as *m*/*z* 196 (isobaric with Si_7^+) and clusters of barium, oxygen, and/or carbon at *m*/*z* 163, 187, and 211 denoted by asterisks; (b) the low mass barium peaks at *m*/*z* 138, 139, and 155; and (c) additional clusters at *m*/*z* 292, 309, and 317. Note the absence of characteristic ions of the free fatty acid at *m*/*z* 295 and 313. The ion fluence is 10^{10} cm^{-2}.

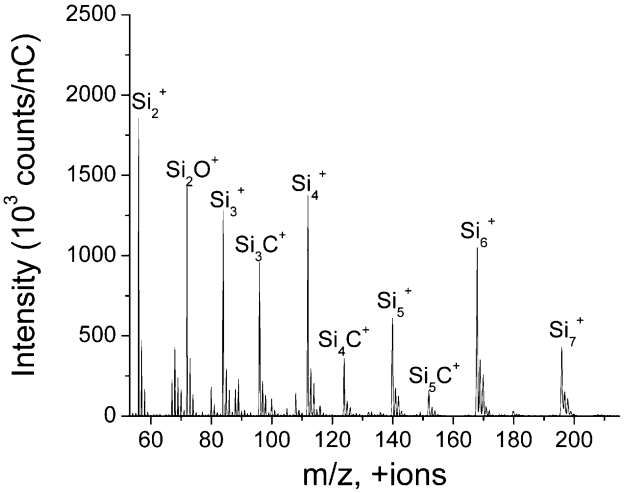

Figure 4. C_{60}^+-induced mass spectrum (ion fluence of 10^{10} cm^{-2}) of the bare silicon surface after C_{60}^+ bombardment (ion fluence of 10^{13} cm^{-2}).

the barium isotope pattern; therefore, the characteristic fragment ion at *m*/*z* 209 is corrected for the contribution of $(BaO_3C_2H)^+$ in all secondary ion yields reported for this fragment. Characteristic neutral fatty acid peaks at *m*/*z* 313 $(M + H)^+$ and *m*/*z* 295 $(M + H - 18)^+$ are not present in the spectrum of the fatty acid salt (Figure 3c). The absence of these fragments and the absence of the L_2 phase in the isotherm (Figure 1b) confirm the conversion of the fatty acid to the fatty acid salt. In a similar fashion, Wandass et al. reported the absence of the $(M + H)^+$ and $(M + H - 18)^+$ peaks and the presence of the barium-cationized peak for barium stearate films, indicating conversion to the fatty acid salt.[28] Negative TOF-SIMS spectra of arachidic acid and barium arachidate result in a molecule specific peak at *m*/*z* 311 $(CH_3(CH_2)_{18}COO^-)$. All analysis to follow is of positive spectra due to sample charging in the negative ion mode.

C_{60}^+ Ion Fluence Dependence. The original (static) C_{60}^+ SIMS spectra measured for the barium arachidate films with varying thickness do not show significant qualitative differences. On the other hand, if the samples are subjected to ion fluences beyond the static limit, changes in the spectra that relate to ion bombardment-induced modification and sputter erosion of the films are observed. By following the primary ion fluence, dependence of characteristic ions for the LB films and the silicon substrate, a depth profile analysis of the LB film is performed. The interesting question in this context is to what extent the molecular information can be preserved during such an analysis.

The film/substrate interface is denoted by the appearance of the silicon substrate. As seen in Figure 4, the silicon substrate can be characterized by many cluster ions. The appearance of the silicon cluster Si_4^+ at *m*/*z* 112 is used to determine the film/substrate interface, since the signal for Si^+ at *m*/*z* 28 appears in

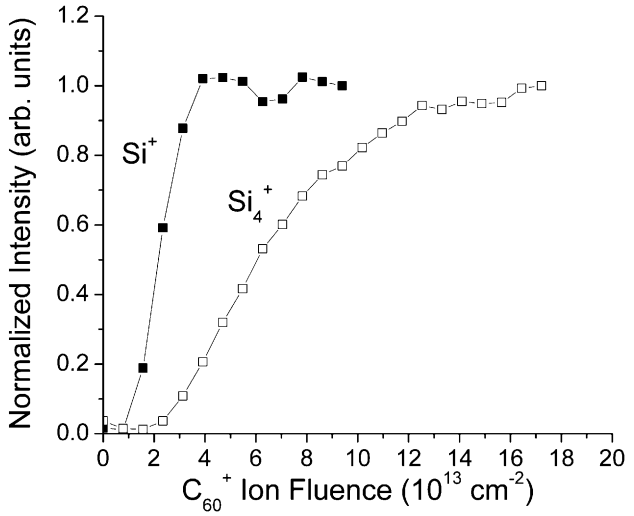

Figure 5. C_{60}^+ ion fluence dependence of Si^+ at *m*/*z* 28 and Si_4^+ at *m*/*z* 112 of a 7-layer barium arachidate LB film. Data acquisition was performed with a C_{60}^+ ion fluence of 10^{10} cm^{-2}.

some cases to be disturbed by isobaric hydrocarbon interferences. The C_{60}^+ fluence dependences of Si^+ at *m*/*z* 28 and Si_4^+ at *m*/*z* 112 are displayed for a 7-layer film in Figure 5. The Si^+ signal is obtained from the part of the peak that is below the nominal mass to avoid hydrocarbon interferences. It is evident that the Si_4^+ signal rises later than the atomic Si^+ signal. This finding is understandable from the formation mechanism of sputtered clusters. While the Si^+ signal should follow the silicon surface concentration, the emission of Si_4^+ requires the presence of four neighbored Si surface atoms and will therefore show a different dependence on that quantity. To locate the interface, we determine the ion fluence at which the Si_4^+ signal starts to rise and has reached ~5% of its maximum value, which roughly coincides with 50% of the maximum signal of *m*/*z* 28 (Figure 5).

For samples containing 1, 7, and 15 layers of barium arachidate, the C_{60}^+ fluence dependence of the $CH_2CHCOOBa^+$ fragment ion at *m*/*z* 209 is displayed in Figure 6a. This dependence appears to closely represent the depth structure of the LB film. For the 1-layer sample, the signal simply falls due to rapid sputter removal of the film. For the 7- and 15-layer films, the signal is initially found to slightly increase and then reach a plateau in the 15-layer case. At fluences of several 10^{13} cm^{-2}, the LB film-related fragment ion signal is found to decrease and finally disappear. At the time the fragment ion disappears, signals arising from the silicon substrate appear (Figure 6b), indicating the complete sputter-removal of the LB film.

From the data presented in Figure 6, the total C_{60}^+ ion fluence required to remove the complete overlayer, indicated by the rise in the Si_4^+ signal, is shown to depend on the initial thickness of the LB film. Using this value in connection with the known initial film thickness, we determine the sputter rate of the film in nm/s. The sputter rate increases 2-fold from 1 to 7 layers and 3-fold from 1 to 15 layers, which implies that the total sputter yield is increasing with film thickness. The respective sputter yields for the 1-, 7-, and 15-layer films are 57, 150, and 190 molecules per incident ion. This trend most likely results because a larger fraction of the collision cascade induced by the projectile impact occurs in the overlayer of the thicker films.

Sputter Yields. The depth profile of a 7-layer film with C_{60}^+ was compared to that of Ga^+. Due to the low secondary ion yields obtained with Ga^+, mass spectral data shown was in all cases acquired with C_{60}^+. The Si_4^+ profiles for Ga^+ and C_{60}^+ bombardment are shown in Figure 7. In both cases, the position of the interface can be clearly determined from the rise of the Si_4^+ signal. The total sputter yield is determined from the ion fluence needed to remove the complete overlayer. The removal of the LB overlayer with Ga^+ bombardment (Figure 7a) requires an ion fluence of 3.2×10^{15} cm^{-2}. This is ~2 orders of magnitude larger than the value of 2.3×10^{13} cm^{-2} obtained for C_{60}^+ bombardment (Figure 7b). From the density of the arachidic acid molecule (1.85×10^{21} molecules/cm^3), the thickness measured by ellipsometry (19 nm), and the bombarded surface area, the number of removed molecules can be determined to be 1.0×10^{13} for the Ga^+ experiment and 8.8×10^{12} for the C_{60}^+ experiment. Therefore, 1.1 molecules are removed for every Ga^+ and 150 molecules for every C_{60}^+ projectile ion impact.

Using the erosion rate in connection with the ion fluence, the Si_4^+ profiles shown in Figure 7 for the 7-layer film can be converted from an ion fluence scale to a depth scale for both the Ga^+ (0.017 nm/s) and C_{60}^+ (1.1 nm/s) bombardment cases, assuming a constant sputter rate throughout the entire sample. The resulting Ga^+ and C_{60}^+ depth profiles displaying the behavior of the ions at *m*/*z* 449 and at *m*/*z* 209 are shown in Figure 8 a and b, respectively. Molecule-specific information is shown to be retained

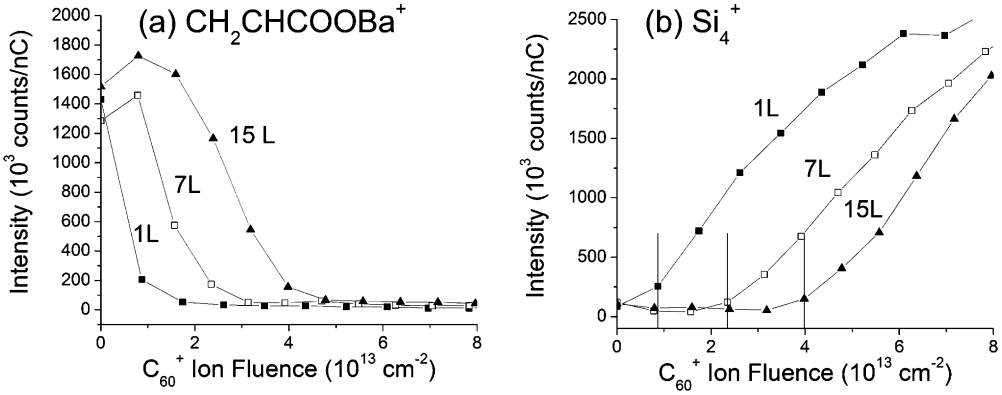

Figure 6. Depth profiles for 1-, 7-, and 15-layer films of barium arachidate depicting (a) the C_{60}^+ ion fluence dependence of the characteristic fragment ion at *m*/*z* 209 and (b) the C_{60}^+ ion fluence required to reach the substrate denoted by Si_4^+ at *m*/*z* 112. Data acquisition was performed with a C_{60}^+ ion fluence of 10^{10} cm^{-2}.

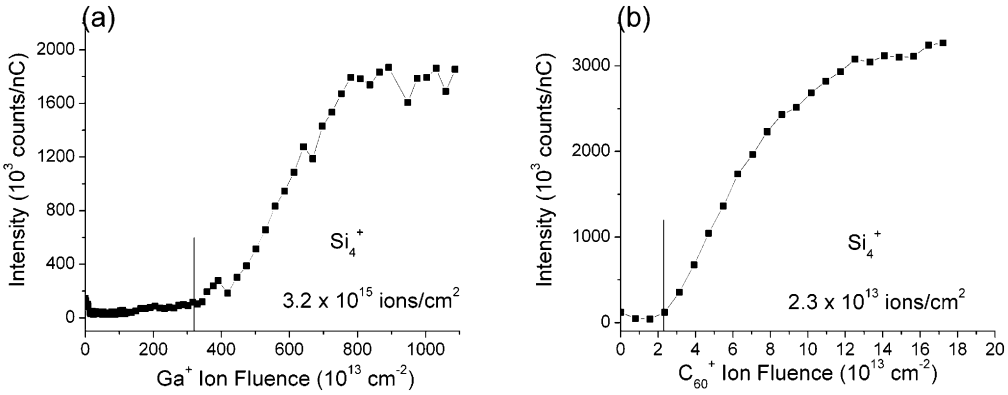

Figure 7. Ion fluence required to remove a 7-layer barium arachidate film on a SiO_2/Si substrate monitored by the presence of the Si_4^+ signal at *m*/*z* 112 for (a) Ga^+ and (b) C_{60}^+ bombardment. Analysis was performed with a C_{60}^+ ion fluence of 10^{10} cm^{-2}.

to the interface (19 nm) with C_{60}^+ bombardment but not with Ga^+ bombardment, confirming the benefits of cluster sources for molecular depth profiling. This is further emphasized in the C_{60}^+ depth profile of the 15-layer film, as shown in Figure 8c. Bombardment with Ga^+ results in a low sputter yield and a rapid loss of characteristic ion signals during sputter removal of the LB film, that is, before signal from the substrate appears at much higher primary ion fluences. This implies that the loss of molecule-specific information is generated by accumulation of ion beam-induced chemical damage.

The interface width can be determined from the fluence between the points where the *m*/*z* 209 fragment ion signal reaches 84% and 16% of its initial or plateau value. The resulting interface width was determined to be 10 nm for the 7-layer film and 19 nm for the 15-layer film, both sputtered with C_{60}^+. This interface width may arise from a number of causes, including interlayer mixing and/or surface effects.

Secondary Ion Yields. In addition to an enhancement in sputter yield, there is also an enhancement in secondary ion yield with the use of the C_{60}^+ source. To determine the yield enhancement for the secondary ions detected here, the respective signals are integrated over the TOF peaks. The results are displayed in Figure 9. The barium-cationized arachidate ion yield (*m*/*z* 449) is enhanced by ~2 orders of magnitude when analyzed with the C_{60}^+ ion source in comparison to the Ga^+ ion source. Furthermore, the enhancement increases with an increasing number of layers of the film. More specifically, both ion yields decrease with increasing thickness, but the decrease with Ga^+ is greater than that found with C_{60}^+. This finding can be explained in terms of different desorption mechanisms induced by the two ion beams. Computer simulations of 15-keV Ga and C_{60} bombardment of a Ag{111} crystal at normal incidence have shown that the impinging C_{60} cluster deposits its kinetic energy closer to the surface than the Ga atom and that the Ga atom penetrates deep into the sample, resulting in damage and a low sputter yield.[41,42] These simulations agree well with our data presented here (Figures 8 and 9). For the case of a monolayer on silicon, the impinging Ga projectile efficiently penetrates the LB film and strongly interacts

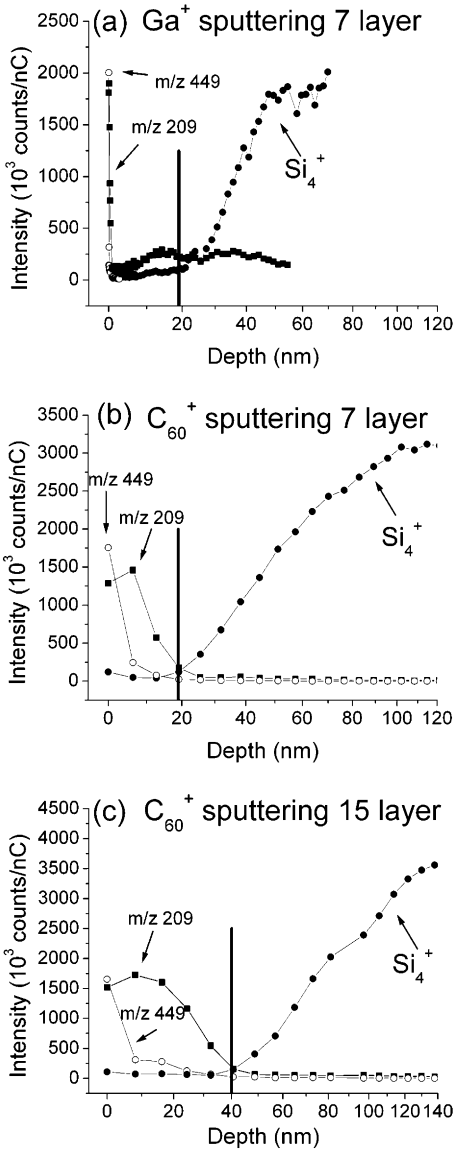

Figure 8. Depth profiles of the fragment ion at *m*/*z* 209 (■) and the barium-cationized arachidate ion at *m*/*z* 449 (○) for 7- and 15-layer barium arachidate films depicting the film/silicon (●) interface at 19 and 40 nm, respectively. Depth profiles resulting from Ga^+ bombardment are represented in (a); those of C_{60}^+ are represented in (b) and (c). Analysis was performed in all cases with a C_{60}^+ ion fluence of 10^{10} cm^{-2}.

(41) Postawa, Z.; Czerwinski, B.; Szewczyk, M.; Smiley, E. J.; Winograd, N.; Garrison, B. J. *Anal. Chem.* **2003**, *75*, 4402−4407.
(42) Postawa, Z.; Czerwinski, B.; Szewczyk, M.; Smiley, E. J.; Winograd, N.; Garrison, B. J. *J. Phys. Chem. B* **2004**, *108*, 7831−7838.

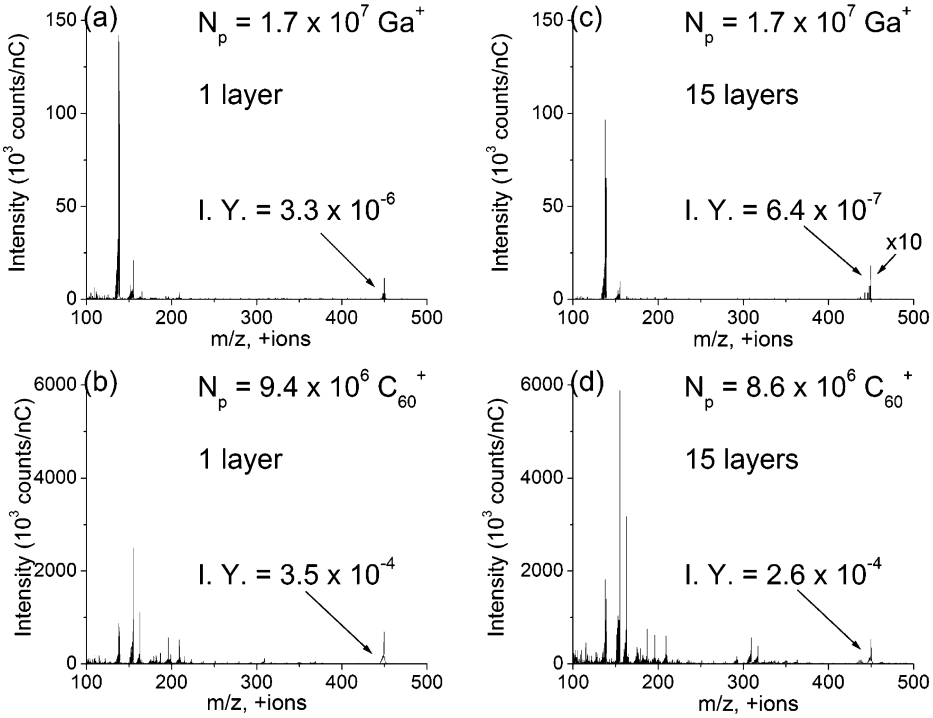

Figure 9. Secondary ion yields (I.Y.) calculated as an integral over the barium-cationized molecular ion peak at *m*/*z* 449 divided by the total number of incident primary ions (N_p) used to accumulate the displayed spectra. (a) Ga^+ bombardment of a 1-layer film, (b) C_{60}^+ bombardment of a 1-layer film, (c) Ga^+ bombardment of a 15-layer film (440−450 amu was multiplied by 10), and (d) C_{60}^+ bombardment of a 15-layer film.

with the silicon substrate. Part of the kinetic energy deposited in the substrate is utilized for molecular desorption from the overlying film. The efficiency of this desorption mechanism will decrease with increasing overlayer thickness, leading to a reduction of the secondary ion yield. Moreover, the energy transfer between projectile constituents and organic molecules is presumably more efficient for impinging C atoms than for a Ga projectile.

The general ion yield enhancement observed here for LB films is similar to the results obtained with softer targets, as reported by Xu et al., who studied the signal of biotin on polystyrene beads with both C_{60}^+ and Ga^+.[19] With C_{60}^+ projectiles, the biotin signal originating from a polystyrene bead surface was more intense than the signal at *m*/*z* 28 for the silicon substrate. In contrast, Ga^+ bombardment gave better signal at *m*/*z* 28 for the silicon substrate. This enhancement with thickness has also been observed for a comparison of SF_5^+ and Ar^+ bombardment.[9] All of these observations indicate that a greater enhancement is achieved when bombarding softer, preferably organic, targets with C_{60}^+.

In comparing the signal enhancement of C_{60}^+ bombardment versus Ga^+ bombardment of the barium arachidate LB films for different secondary ions, it is found that the fragment ion at *m*/*z* 209 is enhanced to a slightly greater extent than the molecular ion at *m*/*z* 449. For the 1-layer film, the fragment ion yield is 200-fold larger for *m*/*z* 209, as compared to 100-fold for the molecular ion. For the 15-layer film, the enhancement factor is 600 for *m*/*z* 209, as compared to 400 for *m*/*z* 449. The reason behind these differences is unknown. Apparently, either the fragmentation mechanism or the ionization of the fragments must be more efficient under C_{60}^+ bombardment as compared to Ga^+ bombardment. Both effects can in principle be caused by the larger surface energy density generated under C_{60} impact.

It has been speculated that the secondary ion yield enhancement associated with cluster bombardment is due to an increase in the respective sputter yield rather than an enhanced ionization probability of the emitted species.[10] For our case, the molecular ion at *m*/*z* 449 emitted from a 7-layer sample is enhanced 200-fold while the total sputter yield is increased by a factor of 140. This result suggests that the ionization probability of the emitted species would be enhanced by a factor of only 1.4. Hence, the secondary ion yield enhancement arises mainly from an overall increase of sputtered material per incident projectile rather than an enhancement of the ionization probability.

CONCLUSION

Our results demonstrate the use of cluster primary ion beams, in particular, a C_{60}^+ ion source, for TOF-SIMS analysis of multilayer LB fatty acid salt films. Depth profile analysis with both cluster and atomic primary ion beams with comparable impact energy demonstrates higher sputter yields of organic samples with cluster sources. The secondary ion yield is enhanced to a greater degree for thicker samples. From a comparison of both effects, the secondary ion yield enhancement is seen to be predominantly due to an increased sputter yield rather than an increase in ionization probability. The fatty acid salt films investigated here represent an intriguing case, since they serve as model systems for biological samples. Hence, the use of C_{60}^+ or similar cluster projectiles opens up a range of new possibilities with respect to the TOF-SIMS analysis of biological systems. Of special interest would be the ability to acquire a three-dimensional molecular characterization of such samples with high spatial resolution.

ACKNOWLEDGMENT

Financial support from the National Institutes of Health and the National Science Foundation is greatly acknowledged. The authors acknowledge Dr. David L. Allara and his research group for the use of the ellipsometer and helpful discussions and Dr. Aapi Sinkkanen for assistance in LB film theory. The authors also thank Dr. A. Daniel Jones, Dr. John C. Vickerman, and Zihua Zhu for their assistance in mass spectral interpretation; Juan Cheng for valuable conversations; and Dr. Zbigniew Postawa for helpful insights into the explanation of data.

Received for review May 19, 2004. Accepted August 27, 2004.

AC0492665